

Optimal Equivalent Circuits for Interconnect Delay Calculations Using Moments *

Andrew B. Kahng and Sudhakar Muddu

UCLA Computer Science Department, Los Angeles, CA 90024-1596 USA

Abstract

In performance-driven interconnect design, delay estimators are used to determine both the topology and the layout of good routing trees. We address the class of *moment-matching*, or *moment representation*, methods used to simulate interconnects modeled as distributed *RC* or *RLC* lines. We provide accurate 2- and 3-segment equivalent circuits for the distributed *RLC* and distributed *RC* models. Our equivalent circuits approximate a distributed *RLC* structure accurately up to second degree terms. We have evaluated our models using the two-pole methodology for voltage response calculations. Previous approximate two-pole approaches have at least 14% error even for small test cases. As routing trees become bigger and interconnection lines become longer, our approach has greater advantages in both accuracy and simulation complexity.

1 Overview

Accurate calculation of propagation delay in VLSI interconnects is critical to the design of high speed systems. Direct simulation codes such as SPICE can fail to afford the efficiency or the physical intuition needed for layout-level design. On the other hand, simple lumped or “distributed-lumped” models become less accurate for interconnect delay estimation as operating frequencies approach the order of GHz (lumped and distributed *RC* models are reviewed in [12, 6]).

In this paper, we develop new segmented interconnect representations for delay simulation in interconnect trees; our goal is to improve both accuracy and efficiency over existing methodologies. Our work is aimed at the class of *moment matching* simulation approaches, which provide acceptable accuracy while maintaining computational efficiency. Traditionally, uniformly lumped segment models (e.g., **L**, **T** or **Π** circuits) are used for modeling interconnect lines [9, 20]. For such *uniform* representations, the moments are perfectly captured only as the number of segments used approaches infinity. With any finite number of segments, the moments will be either underestimated or overestimated depending on the type of segment (**L**, **T** or **Π**).

In this paper, we develop very accurate *non-uniform equivalent circuits* for both the distributed *RC* and the distributed *RLC* transmission line models. This concept is originally due to Rajput [14], who proposed a model with two non-uniform **L** segments to approximate the response of a distributed *RC* line. For a step input, the

response of Rajput’s equivalent circuit is within 3% of the correct response. The equivalent circuit also matches *exactly* the first two moments of the distributed *RC* line (i.e., the transfer function matches that of the distributed *RC* line up to the coefficient of s^2); such an equivalent circuit is *optimal* in terms with respect to the first two moments and the moment-matching methodology. Because the two non-uniform **L** segments achieve the exact accuracy that would require an infinite number of uniform **L** segments, simulation time is greatly reduced. Gerzberg [5] surveyed different non-uniform models and proposed a model in which the segment *RC* values are in geometric progression (the “Uniform Distributed RC” (URC) line model in SPICE is derived from Gerzberg’s model). Non-uniform equivalent circuits have also been used in other areas, e.g., Gopal et al. [7] obtain a non-uniform segment model for driving-point impedance at a gate output using moment-matching techniques.¹ To evaluate the effect of our equivalent circuits in the context of previous moment-based methods, we employ the two-pole method of Zhou et al. [20] and obtain the voltage response for a small tree network studied in [20]. We show that the delay calculations in [20] have over 14% error for this instance.

2 Background: Moment Matching

In a linear system, the transfer function $H(s) = \frac{V_{out}(s)}{V_{in}(s)}$ gives the relationship between the output response $V_{out}(s)$ and the input response $V_{in}(s)$. Let $h(t)$ be the impulse response corresponding to the transfer function. Without loss of generality, the transfer function for any linear system can be expressed as a ratio of polynomials in s , that is to say,

$$H(s) = K \frac{1 + a_1s + a_2s^2 + a_3s^3 + \dots}{1 + b_1s + b_2s^2 + b_3s^3 + \dots} \quad (1)$$

where K is the *DC* (zero frequency) gain. The i^{th} moment of the linear system is defined as

$$M_i = \frac{1}{i!} \int_0^\infty t^i h(t) dt = \frac{(\Leftrightarrow 1)^i}{i!} H^{(i)}(0) \quad (2)$$

where $H^{(i)}(0)$ is the i th derivative of $H(s)$ at $s = 0$.

Assuming $v_{out}(0) = 0$, the Laplace transform of the derivative of the output voltage response for a unit step

¹Sakurai [17] has observed that the use of such an equivalent circuit is not always appropriate since it cannot predict the correct response when the line is driven bidirectionally. However, in most routing tree design problems the direction of signal flow is known.

*This work was supported by NSF MIP-9257982. The work of ABK was supported in part by NSF MIP-9117328 during a Spring 1993 sabbatical visit to UC Berkeley.

input is $v'_{out}(t) \Leftrightarrow sV_{out}(s) = s \cdot \frac{1}{s}H(s) = H(s) \Leftrightarrow h(t)$. Therefore, the transfer function can also be written as

$$H(s) = \int_0^{\infty} e^{-st} v'_{out}(t) dt.$$

Expanding e^{-st} into a Maclaurin series,

$$H(s) = \int_0^{\infty} v'_{out}(t) dt \Leftrightarrow \frac{s}{1!} \int_0^{\infty} t v'_{out}(t) dt + \frac{s^2}{2!} \int_0^{\infty} t^2 v'_{out}(t) dt \Leftrightarrow \frac{s^3}{3!} \int_0^{\infty} t^3 v'_{out}(t) dt + \dots,$$

and identifying the integral quantities as moments M_0, M_1, M_2, M_3 etc. from Equation (2), we get

$$H(s) = (M_0 \Leftrightarrow sM_1 + s^2M_2 \Leftrightarrow s^3M_3 + \dots).$$

The relationships among the moment representation, the Laplace transform of the response, and the time-domain response are very well discussed in [13].

3 Uniform Segment Models

For any RLC network, the coefficients a_i and b_i of the transfer function are in terms of the R, L, C circuit parameters [10]. Here, we first seek simple equivalent circuits for the case of the open-ended distributed transmission line. The $ABCD$ parameters of a distributed RLC transmission line (Figure 1), are [3]:

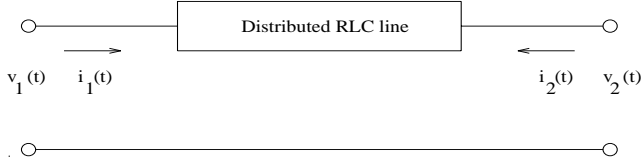


Figure 1: 2-port distributed RLC line model.

$$\begin{pmatrix} V_1(s) \\ I_1(s) \end{pmatrix} = \begin{pmatrix} \cosh(\theta h) & Z_0 \sinh(\theta h) \\ \frac{1}{Z_0} \sinh(\theta h) & \cosh(\theta h) \end{pmatrix} \begin{pmatrix} V_2(s) \\ I_2(s) \end{pmatrix} \quad (3)$$

where $\theta = \sqrt{(r + sl)sc}$, h = length of the line and $r = \frac{R}{h}$, $l = \frac{L}{h}$ and $c = \frac{C}{h}$ are the resistance, inductance and capacitance per unit length. Since $I_2(s) = 0$ for an open-ended distributed RLC line, the voltage response at the end of the line is $V_2(s) = \frac{V_1(s)}{\cosh(\theta h)}$. Therefore, the numerator polynomial of the open-ended transfer function is a constant (all a 's = 0) and we have

$$H(s) = \frac{1}{\cosh(\sqrt{(R + sL)sC})} = \frac{1}{1 + \frac{RC}{2}s + \left(\frac{(RC)^2}{24} + \frac{LC}{2}\right)s^2 + \left(\frac{(RC)^3}{720} + \frac{RLC^2}{12}\right)s^3 + \dots}$$

Analogous results for the distributed RC line are obtained by substituting $L = 0$ in the above equation. We now discuss the **L** and **T** models, which have traditionally been used to approximate the distributed transmission line. The **II** model analysis is similar to that of the **T** model.

3.1 Uniform L Segments

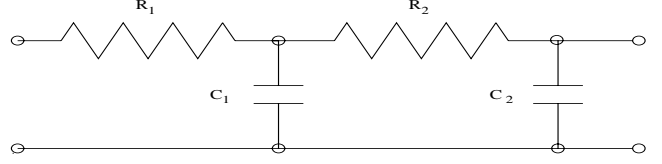


Figure 2: Two uniform **L** segments model.

The open-ended transfer function for two uniform **L** segments (Figure 2) is

$$H_{2L}(s) = \frac{1}{1 + s(R_1(C_1 + C_2) + R_2C_2) + s^2R_1R_2C_1C_2}$$

Substituting $R_1 = R_2 = R/2$ and $C_1 = C_2 = C/2$ yields

$$H_{2L}(s) = \frac{1}{1 + \frac{3RC}{4}s + \frac{(RC)^2}{16}s^2} \quad (4)$$

Coefficients for the three uniform **L** segments model are given in Table 1. As the number of segments tends to infinity, the **L** type model approaches the RC distributed line model given in Equation (4) with $L = 0$. In [10], we prove that as $N \rightarrow \infty$, b_1 , b_2 and b_3 all tend to their respective values given in Equation (4).²

3.2 Uniform T Segments

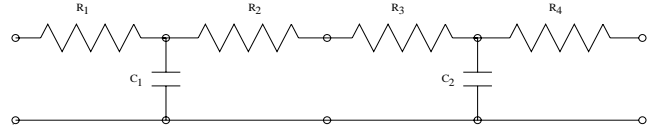


Figure 3: Two uniform **T** segments model.

The open-ended transfer function for two uniform **T** segments (Figure 3) is

$$H_{2T}(s) = \frac{1}{1 + s(R_1(C_1 + C_2) + (R_2 + R_3)C_2) + s^2R_1(R_2 + R_3)C_1C_2}$$

Substituting $R_1 = R_2 = R_3 = R_4 = R/4$ and $C_1 = C_2 = C/2$ yields

$$H_{2T}(s) = \frac{1}{1 + \frac{RC}{2}s + \frac{(RC)^2}{32}s^2} \quad (5)$$

Coefficients for the three uniform **T** segments model are given in Table 1. Sakurai [17] showed that for both the

²Interestingly, the coefficient b_3 is not monotone with respect to the number of segments: b_3 is close to its optimal value of $1/720$ when there are three uniform segments; the maximum error is achieved with seven segments before decreasing [10]. As an example, using 10 uniform segments to approximate the distributed RLC line entails error in the coefficient b_3 of approximately 25% (at the same time, the error in b_1 is around 10% and that of b_2 is 20%). The corresponding errors in the first moment and second moment are 10% and 20%, respectively.

T and **II** models, as the number of segments tends to infinity all the coefficients will converge to their respective values in Equation (4). We can see that for any finite number of segments, the uniform **T** segments **underestimate** the coefficient of s^2 in the denominator of the transfer function, while the uniform **L** segments **overestimate** the coefficients of s and s^2 . A comparison of various lumped models for the distributed RC line can be obtained by substituting $L = 0$ in the Table 1 coefficients.

Method	b_1	b_2	b_3
Dist. RLC Line Model	$\frac{RC}{2}$	$\frac{(RC)^2}{24} + \frac{LC}{2}$	$\frac{(RC)^3}{720} + \frac{RLC^2}{12}$
2 U L	$\frac{3RC}{4}$	$\frac{(RC)^2}{16} + \frac{3LC}{4}$	$0 + \frac{RLC^2}{8}$
3 U L	$\frac{2RC}{3}$	$\frac{5(RC)^2}{81} + \frac{LC}{2}$	$\frac{(RC)^3}{729} + \frac{10RLC^2}{81}$
2 U T	$\frac{RC}{2}$	$\frac{(RC)^2}{32} + \frac{LC}{2}$	$0 + \frac{RLC^2}{16}$
3 U T	$\frac{RC}{2}$	$\frac{(RC)^2}{27} + \frac{LC}{2}$	$\frac{(RC)^3}{145.8} + \frac{2RLC^2}{27}$
2 non-U L	$\frac{RC}{2}$	$\frac{(RC)^2}{24} + \frac{LC}{2}$	$0 + \frac{RLC^2}{12}$
3 non-U L	$\frac{RC}{2}$	$\frac{(RC)^2}{24} + \frac{LC}{2}$	$\frac{(RC)^3}{1111.11} + \frac{RLC^2}{12.02}$

Table 1: Various models approximating the open-ended transfer function of distributed RC (having $L = 0$) and RLC lines. We use U / non-U to indicate uniform / non-uniform.

4 Non-Uniform Segment Models

Rajput [14] proposed the following equivalent circuit, composed of two non-uniform **L** segments, for an open-ended distributed RC line. With respect to Figure 2, Rajput's circuit has element values

$$R_1 = \frac{1}{4}R, \quad R_2 = \frac{3}{4}R; \quad C_1 = \frac{2}{3}C, \quad C_2 = \frac{1}{3}C$$

and its open-ended transfer function is

$$H_{Raj_2}(s) = \frac{1}{1 + \frac{RC}{2}s + \frac{(RC)^2}{24}s^2} \quad (6)$$

Thus, the open-ended transfer function of a distributed RC line (Equation (4)) is captured **exactly** up to the coefficient of s^2 , i.e., the first two moments are exact. Rajput obtained these values by comparing the transfer function and input impedance of the equivalent circuit with those of the distributed RC line. In this section we will calculate non-uniform equivalent circuits, under the open-ended assumption, to approximate the higher moments; we then extend the technique to obtain RLC models.

4.1 RC Segment Model

For three non-uniform **L** segments, as shown in Figure 4, we solve for the resistance and capacitance values by calculating the open-ended transfer function and the open-circuit input impedance; this leads to 7 equations with 6 unknowns, an overspecified system [10]. Since

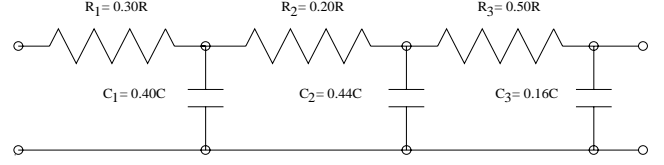


Figure 4: Three non-uniform **L** segments model.

there are no solutions to this system of equations, we use numerical search techniques to minimize the squared error in the b_1 , b_2 and b_3 values. We thus obtain the circuit parameters

$$R_1 = 0.30R, \quad R_2 = 0.20R, \quad R_3 = 0.50R$$

$$C_1 = 0.40C, \quad C_2 = 0.44C, \quad C_3 = 0.16C$$

The values of the corresponding coefficients of s 's in the transfer function are extremely close to the exact values given in Equation (4); again, note that just three segments, rather than a large number of segments, can achieve this accuracy. The contrast with the various uniform RC models used to model the transmission line can be seen by substituting $L = 0$ in Table 1. Further, it should be noted that non-uniform RLC equivalent circuits can be used to model distributed RC lines. For example, a single RLC circuit with $R_1 = \frac{R}{2}$, $C_1 = C$, and $L_1 = \frac{R^2C}{24}$ can be used to approximate the distributed RC line up to the coefficient of s^2 .

4.2 RLC Segment Models

Extending the equivalent-circuit technique to the distributed RLC line is straightforward (see [10]). For two non-uniform RLC segments (Figure 5), we obtain the following values for the circuit elements:

$$R_1 = \frac{1}{4}R, \quad R_2 = \frac{3}{4}R$$

$$L_1 = \frac{1}{4}L, \quad L_2 = \frac{3}{4}L$$

$$C_1 = \frac{2}{3}C, \quad C_2 = \frac{1}{3}C$$

The open-ended transfer function for this model is

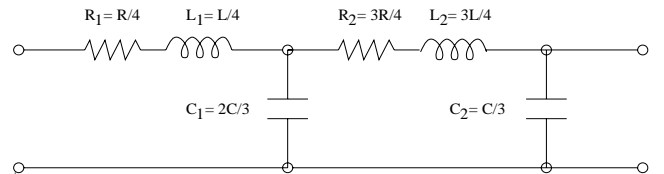


Figure 5: Two non-uniform **L** segments model.

$$H(s) = \frac{1}{1 + \frac{RC}{2}s + \left(\frac{(RC)^2}{24} + \frac{LC}{2}\right)s^2 + \frac{RLC^2}{12}s^3} \quad (7)$$

and comparing Equation (7) to Equation (4), shows that two non-uniform RLC segments can obtain the first and

second moments exactly. We have also numerically optimized an equivalent circuit with three non-uniform RLC segments. The optimized circuit elements are

$$\begin{aligned} R_1 &= 0.30R, & R_2 &= 0.20R, & R_3 &= 0.50R \\ L_1 &= 0.30L, & L_2 &= 0.20L, & L_3 &= 0.50L \\ C_1 &= 0.40C, & C_2 &= 0.44C, & C_3 &= 0.16C \end{aligned}$$

and this non-uniform three-segment RLC model captures the first two moments exactly, and the third moment almost exactly. Notice that the resistance and inductance values are distributed identically because they have to satisfy similar equations in matching the coefficients. From Table 1, it is clear that the use of such non-uniform equivalent circuits in a two-pole or higher-order approximation of the transfer function will a more accurate voltage response than the uniform segment models used in, e.g., [20].

4.3 Complexity Reduction

For large routing trees, using non-uniform equivalent circuits for a distributed RLC line will reduce the computation time significantly when compared with using a number of uniform RLC segments. Such works as [16] or [20] suggest using k segments to model each interconnect line; for large MCM interconnects the appropriate value of k can be quite large. Let N be the total number of interconnect lines between a given input node and output node. From the expressions given in [10], the computation time of b_1 is of the order of $O((kN)^2)$, that of b_2 is on the order of $O((kN)^4)$ and that of b_3 is $O((kN)^6)$. By using two non-uniform segments the computation time will be reduced to $O(N^2)$ for b_1 , $O(N^4)$ for b_2 and $O(N^6)$ for b_3 , which corresponds to a substantial reduction if the interconnection tree is large or if accuracy is desired.

5 Two-Pole Methods for Tree Analysis

5.1 Previous Methods

Horowitz [9] proposed a method for estimating the response and delay through RC trees using both single-pole and two-pole methods: he calculates the poles of the estimated system response from the first and second moments of the main path (i.e., the unique path from the input node to the output node) in the RC tree. His paper with Rubinstein et al. [16] suggests that for delay analysis of RC trees, each distributed RC line should be replaced by a finite number of lumped RC segments to achieve the required accuracy.³

Zhou et al. [19] proposed an analytical approach for calculating the dominant poles for a single transmission line by using a *single* RLC segment as the underlying model. The analysis assumes a linear model for the source $I \Leftrightarrow V$ curve, and obtains a polynomial describing the poles of the transmission line. By making various assumptions about this polynomial, the poles of interest are obtained ([19], p. 781). Based on this work, Zhou

et al. [20] then compute poles of a general interconnection tree. Since the polynomial obtained in [19] is based on a single RLC segment, the coefficient of s^2 (i.e., b_2) will not have any $(RC)^2$ term. Based on this model, the voltage response in a general interconnection tree is computed from the two dominant poles. To achieve improved accuracy, the authors of [20] propose modeling each tree branch by many shorter segments (but this deviates from the underlying assumptions in that not every branch of the tree drives the small capacitive load). This method is somewhat impractical when used for trees with long wire segments (e.g., for MCMs). Since the poles are computed by approximating the off-path subtree admittance by the sum of the total subtree admittance (i.e., approximating subtree admittance up to coefficient of s) [20, 8], the response is not exact.

5.2 Experimental Comparisons

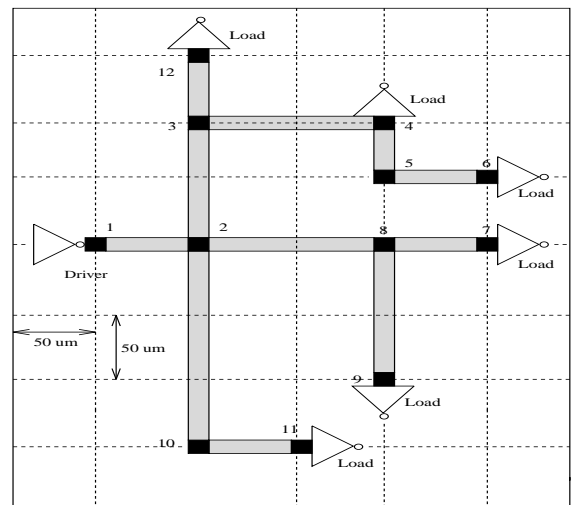


Figure 6: A tree interconnection layout studied in [20].

We now give a practical demonstration of the utility of our non-uniform equivalent circuit models, in the context of the two-pole simulation methodology. For the interconnect tree studied in [20] (see Figure 6), we plot the voltage response at a specific node (Node 6) using each of five distinct simulation methodologies:

- **App2Pole** is the “approximate two-pole” method of Zhou et al. [20] discussed above, wherein the poles of an interconnection tree are heuristically computed and a two-pole analysis is then applied.
- **Stan2Pole** is the standard two-pole approximation for the system transfer function [9, 20],

$$H(s) = \frac{k_1}{s \Leftrightarrow s_1} + \frac{k_2}{s \Leftrightarrow s_2}$$

where s_1, s_2 are the poles and k_1, k_2 are the coefficients corresponding to the poles. Using Laplace transform techniques, one can express both the poles and the coefficients in terms of the first and second

³The first moment (M_1) of the system impulse response corresponds to the delay measure proposed by Elmore [4]; this corresponds to a single dominant pole approximation of the response.

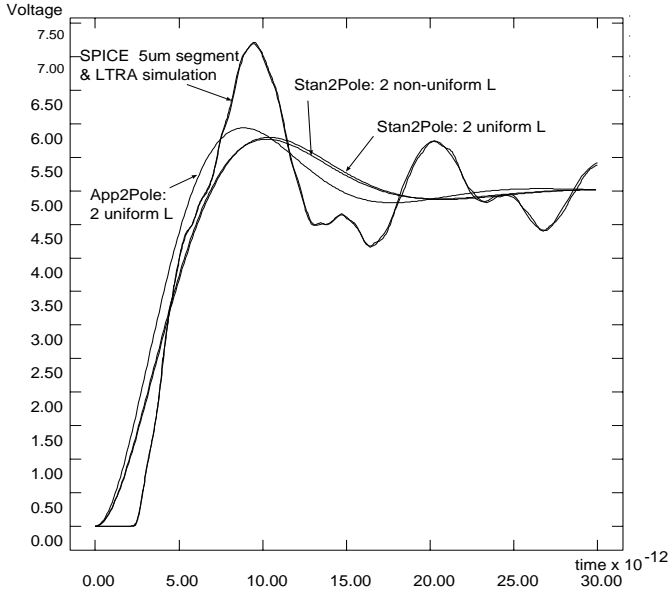


Figure 7: Unit step response at Node 6 of the tree shown in Figure 6, using both uniform and non-uniform models (Stan2Pole), SPICE approaches, and the approximate App2Pole method of [20]. Following [20], the driver resistance is 10Ω .

moments⁴ [10, 20]. The voltage response is then calculated as

$$V_{out}(t) = \left(1 + \frac{k_1}{s_1} e^{s_1 t} + \frac{k_2}{s_2} e^{s_2 t} \right)$$

For the tree analysis using the standard two-pole approximation, we replace each interconnect line by the uniform L segment circuits given in Section 3. We then identify the “main path” from the source to the output (sink) node. The off-path sub-tree impedance is approximated by the total capacitive impedance [20]. The delay thus computed is an upper bound on the exact delay.

- With our new non-uniform segment model, we calculate the voltage response for interconnection trees using the same Stan2Pole methodology, and replacing each interconnect line by a non-uniform equivalent circuit.
- **SPICE** simulation of the interconnect tree can be performed with each interconnect line of the tree divided into a large number of uniform RLC segments, as in [20] [8]. The voltage response so obtained will be exact in the limit (i.e., as the number of RLC segments per interconnect line approaches infinity). We apply this method by dividing each interconnect line into uniform RLC segments of length $5\mu m$.

⁴The poles are $s_{1,2} = \frac{-M_1 \pm \sqrt{4M_2 - 3M_1^2}}{2}$ and the coefficients are $k_1 = -k_2 = -\frac{1}{\sqrt{4M_2 - 3M_1^2}}$.

- Finally, the **LTRA** (Lossy TRANsmission line) model in SPICE models each interconnect line in the tree as a lossy transmission line. This model is also referred to as a uniform transmission line model because it has constant resistance, capacitance and inductance per unit length, uniformly distributed over the length of the line. The LTRA model calculates the response using the convolution of the transmission line’s impulse response with the input response [15]. In the limit, as the number of segments per interconnect line tends to infinity, the SPICE segmented response coincides with that of the LTRA approach.

We plotted the voltage response at Node 6 of the tree interconnection layout studied in [20] (see Figure 6), using using the above approaches and varying driver resistances.

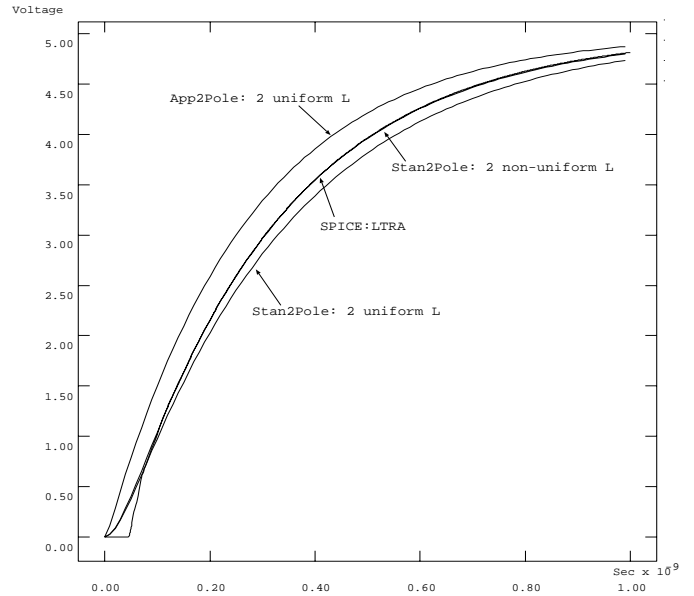


Figure 8: Unit step response at Node 6 of the same tree topology, with the branches (edges) between nodes (1, 2) and between nodes (2, 3) scaled by a factor of 40, and all other branches scaled by a factor of 10. Again, we compare the uniform/non-uniform models using the Stan2Pole method against SPICE simulations and the App2Pole method; driver resistance is 150Ω .

Figure 7 shows the voltage response at Node 6 with a driver resistance of 10Ω . The response calculated using our non-uniform model is fairly comparable with the SPICE simulation, and the response calculated using uniform and non-uniform equivalent circuits is almost identical. However, as the interconnection tree becomes larger the response of the uniform method moves *away* significantly from the SPICE response.

To demonstrate the increase of error for longer interconnects, we used the same tree but scaled the length of edges (1, 2) and (2, 3) by a factor of 40 and all other edge lengths by a factor of 10. The response at Node 6 is given in Figure 8; the error in the 90% threshold

delay between two uniform RLC segments and two non-uniform RLC segments is approximately 14%. We also observe that as more uniform segments per interconnect line are used, the “approximate two-pole” response actually moves *away* from the SPICE response. In contrast, the response calculated using either SPICE simulation methodology is very close to the Stan2Pole result using our non-uniform models. As driver resistance decreases or as wire length increases, the difference between these models becomes much more significant. For high-speed systems or MCM layout applications where the wire lengths become very large, use of our non-uniform segment model will significantly improve accuracy and efficiency versus previous two-pole methods.

6 Conclusions

Accurate estimation of signal propagation delays in interconnects is a major obstacle to correct implementation of high-speed systems. In this paper, we simulate interconnect trees by modeling each distributed interconnect line using accurate non-uniform lumped segment models. Since our non-uniform segment models approximate the moments of the transfer function of the distributed line very accurately using only two or three segments, we obtain improvements in both simulation complexity and accuracy over previous methodologies [9, 20]. We show that the 90% threshold delay estimates of previous work [20] are incorrect by 14% even for a very small routing topology. Such differences are significant for critical timing analyses in the design of high-speed systems, and we believe that non-uniform equivalent circuits can supersede the lumped \mathbf{T} and $\mathbf{\Pi}$ models traditionally used for delay estimation, clock skew minimization and other routing applications. Moreover, the evaluations of existing routing tree techniques (such as Elmore routing trees [1] or A-trees [2]), whose delays were measured using the technique of [20], may change.

In [11], we have developed non-uniform equivalent circuits to model distributed RLC lines with general source and load impedances. In general, the coefficients of the distributed RLC line can be obtained using the recursive expression given in [10]. Similarly, the coefficients of the non-uniform equivalent circuits can be obtained recursively in terms of the equivalent circuit parameters. The parameter values can be derived by matching the coefficients of the transfer function with the non-uniform equivalent circuits (note that Yu and Kuh [18] have also proposed an approach for directly calculating the moments of distributed line, and given a derivation of equivalent circuit parameters). Our current work addresses the exact computation of moments and poles using the recursive admittance formulation for interconnection trees.

Acknowledgments

We would like to thank Professor Ernest S. Kuh of UC Berkeley, Professor Wayne Wei-Ming Dai and Mr. Haifang Liao of UC Santa Cruz, and Dr. Heinz Mattes of Siemens AG for their helpful comments on an early draft of this work.

References

[1] K. D. Boese, A. B. Kahng and G. Robins, “High-Performance

Routing Trees With Identified Critical Sinks”, *Proc. 30th ACM/IEEE DAC*, June 1993, pp. 182-187.

[2] J. Cong, K. S. Leung and D. Zhou, “Performance-Driven Interconnect Design Based on Distributed RC Delay Model”, *Proc. 30th ACM/IEEE DAC*, June 1993, pp. 606-611.

[3] L. N. Dworsky, *Modern Transmission Line Theory and Applications*, Wiley, 1979.

[4] W. C. Elmore, “The Transient Response of Damped Linear Networks with Particular Regard to Wideband Amplifiers”, *J. Applied Physics* 19, Jan. 1948, pp. 55-63.

[5] L. Gerzberg, “Monolithic Power-Spectrum Centroid Detector”, *PhD Thesis*, Stanford University, May 1979.

[6] M. S. Ghauri and J. J. Kelly, *Introduction to Distributed-Parameter Networks: With Application to Integrated Circuits*, New York: Holt, Rinehart and Winston, 1968.

[7] N. Gopal, Dean P. Neikirk and L. T. Pillage, “Evaluating RC-Interconnect Using Moment-Matching Approximations”, *Proc. ICCAD*, Jun. 1991, pp. 74-77.

[8] D. S. Gao and D. Zhou, “Propagation Delay in RLC Interconnection Networks”, *Proc. IEEE ISCAS*, May 1993, pp. 2125-2128.

[9] M. A. Horowitz, “Timing Models for MOS Circuits”, *PhD Thesis*, Stanford University, Jan. 1984.

[10] A. B. Kahng and S. Muddu “Delay Estimation of Trees using Two-pole method and Optimal Equivalent Circuits”, *UCLA CS Dept. TR-930035*, Oct. 1993.

[11] A. B. Kahng and S. Muddu, *submitted manuscript*, April 1994.

[12] U. Kumar, “Modeling of Distributed Lossless and Lossy Structures: A Review”, *IEEE Circuits and Systems Magazine*, 1980, pp. 12-16.

[13] S. P. McCormick, “Modeling and Simulation of VLSI Interconnections with Moments”, *PhD Thesis*, MIT, June 1989.

[14] Y. V. Rajput, “Modelling Distributed RC Lines for the Transient Analysis of Complex Networks”, *Int. J. of Electronics* 36(5), 1974, pp. 709-717.

[15] J. S. Roychowdhury and D. O. Pederson, “Efficient Transient Simulation of Lossy Interconnect”, *Proc. 28th ACM/IEEE DAC*, Jun. 1991, pp. 740-745.

[16] J. Rubinstein, P. Penfield and M. A. Horowitz, “Signal Delay in RC Tree Networks”, *IEEE TCAD*, Jul. 1983, pp. 202-211.

[17] T. Sakurai, “Approximation of Wiring Delay in MOSFET LSI”, *IEEE Journal of Solid-State Circuits*, Aug. 1983, Vol.18, No.4, pp. 418-426.

[18] Q. Yu and E. S. Kuh, “Moment Matching Model of Transmission Lines and Application to Interconnect Delay Estimation”, *manuscript*, 1994.

[19] D. Zhou, F. P. Preparata and S. M. Kang, “Interconnection Delay in Very High-Speed VLSI”, *IEEE Trans. on Circuits and Systems* 38(7), July 1991, pp. 779-790.

[20] D. Zhou, S. Su, F. Tsui, D. S. Gao and J. S. Cong, “A Simplified Synthesis of Transmission Lines With a Tree Structure”, *J. Analog Integrated Circuits and Signal Processing* 5, Jan. 1994, pp. 19-30.